

Peer review status:

This is a non-peer-reviewed preprint submitted to EarthArXiv.

Strategic crop relocation could substantially mitigate nuclear winter yield losses

Simon Blouin^{a,*}, Morgan Rivers^{a,*}, Michael Hinge^a, Mariana Antonietta^a, Ines Jimenez^a, Florian Ulrich Jehn^a, David C. Denkenberger^{a,b}

^a Alliance to Feed the Earth in Disasters (ALLFED)

^b Department of Mechanical Engineering, University of Canterbury, New Zealand

* These authors contributed equally to this work and are listed alphabetically.

Correspondence to: Simon Blouin (simon.b@allfed.info) or David C. Denkenberger (david@allfed.info)

This manuscript is a non-peer-reviewed preprint submitted to EarthArXiv. This manuscript has been submitted to Nature Food.

Nuclear war could inject millions of tonnes of soot into the stratosphere, cooling the Earth and devastating crop yields. We assess crop relocation—switching which crops are grown where—as an adaptation strategy. Using the Mink crop model, we simulate six major crops under three nuclear winter scenarios (16, 47, and 150 Tg of soot). Without adaptation, global caloric production falls 23%, 53%, and 85% respectively during the worst year of each scenario. We find that mild cooling scenarios favor expanding high-calorie warm-season crops like rice and maize, while severe scenarios require extensive conversion to cold-tolerant crops like rapeseed. In the extreme 150 Tg scenario, crop relocation could double food production compared to current planting patterns. While insufficient to prevent widespread famine in severe scenarios, crop relocation has the potential to save billions of lives.

A nuclear exchange targeting cities could ignite numerous firestorms, collectively injecting millions of tonnes of soot into the stratosphere and triggering a nuclear winter that could persist for years¹⁻³. Within weeks to months, global temperatures would plummet before any unprepared agricultural response could be mounted. The resulting combination of severe cooling, reduced precipitation, and attenuated solar radiation would devastate crop production worldwide, threatening the food security of billions^{4,5}. Given persistent tensions between nuclear-armed states, developing agricultural adaptation strategies before such a catastrophe occurs should be an urgent global priority.

Recent modeling efforts have quantified the devastating impacts of nuclear winter on agriculture^{4,6,7}. Xia et al.⁴ found that a 150 Tg soot injection could reduce global crop yields by 90% in the worst year of a nuclear winter, assuming static crop distributions. These studies reveal the vulnerability of current agricultural systems to rapid cooling from nuclear war soot injection but have largely overlooked adaptation strategies beyond cultivar selection^{8,9}.

While maintaining current crop distributions would lead to catastrophic losses, relocating crops—switching which species are grown where—could offer substantial mitigation. Crop relocation is a recurring theme in agricultural history, from the introduction of potatoes in Europe¹⁰ to ongoing shifts in crop distributions in response to contemporary climate change¹¹. Nuclear winter's severe food shortages would likely drive farmers to switch to crops that could yield harvestable calories in altered climates, especially given elevated food prices. However, nuclear winter would demand far more rapid adaptation than historical precedents, with success likely requiring prior preparation.

Here we evaluate global crop relocation as an adaptation strategy for nuclear winter scenarios. Using the Mink global gridded crop model, we simulate yields of six major crops under three nuclear winter scenarios and identify crop distributions that maximize caloric production. Our analysis provides the first comprehensive assessment of inter-species crop switching potential, establishing both its promise and limitations.

Results

Validation against previous nuclear winter assessments To validate our modeling approach, we first simulated the four staple crops analyzed by Xia et al. (maize, wheat, soybean, and rice) using the same climate projections from their nuclear winter scenarios (see Methods). Together, these four crops currently provide almost half of global calories, making them a representative proxy for global agricultural response to nuclear winter conditions. We calculated global caloric production for each crop relative to baseline climate conditions, then aggregated results using weights based on each crop's current contribution to global caloric production^{12,13}. Our simulations show broad agreement with Xia et al.'s projections across all three scenarios, with the most severe impacts around year 3 post-conflict (Fig. 1). The agreement between our DSSAT-based Mink model and Xia et al.'s CLM5crop simulations is reassuring given that crop models are being applied outside the climate regimes for which they were originally parametrized.

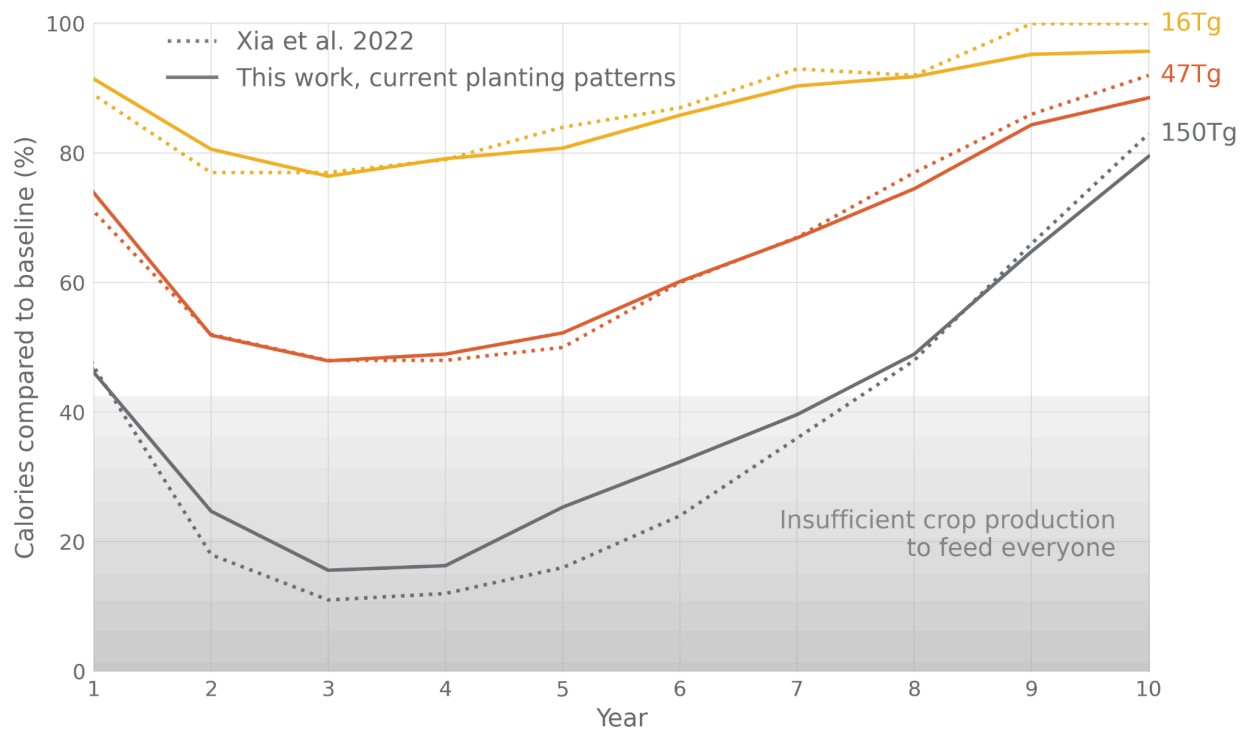


Fig. 1 | Comparison of global caloric production for maize, wheat, soybean, and rice between this work and Xia et al.⁴ The plot shows calories produced compared to pre-war baseline levels (%) over a 10-year period for three soot injection scenarios: 150 Tg (gray), 47 Tg (orange), and 16 Tg (yellow). Solid lines represent results from this work using current planting patterns, while dotted lines show results from Xia et al. The war takes place on 15 May of year 1. The gray shaded area indicates insufficient crop production to feed the global population, assuming 2,300 kcal per person per day (accounting for 10% food waste and redirecting all human-edible crop production from animal feed and biofuel to direct human consumption).

Current global crop production totals 16 quadrillion kcal annually, theoretically sufficient to provide 5,500 kcal per person per day if all production went directly to human consumption⁵. However, with 44% of harvested crops lost to waste, animal feed, and biofuel production, the effective availability for direct human consumption is currently much lower¹⁴. In order to provide intuition about relevant scales of food production, we assume that in a nuclear winter crisis, all human-edible crop production would be redirected away from animal feed and biofuel to direct human consumption^{4,5}. Assuming an average minimum requirement of 2,100 kcal per person per day for basic health¹⁵, and accounting for a reduced waste under crisis conditions of 10% of production⁵, global production would need to maintain at least 2,300 kcal per person per day. This 2,300 kcal/person/day requirement represents 42% of the current 5,500 kcal/person/day crop production.

Assuming the yield response of the four crops modeled in Fig. 1 represents the broader agricultural system, production falls below this 42% threshold for six consecutive years in the 150 Tg scenario, implying widespread famine without additional adaptation measures (existing food stocks would be insufficient^{5,16}). The 47 Tg scenario approaches this threshold during the worst years, while the 16 Tg scenario maintains production well above minimum requirements. However, this global analysis obscures distribution challenges. Historical food crises have shown that even modest production shocks can be amplified by trade disruptions, causing dramatic price increases that place food beyond the reach of vulnerable populations¹⁷. Even in the 16 Tg scenario, regional famines could occur due to failures of food access, despite technically adequate global production.

Crop relocation potential For this analysis, we expanded beyond the four staple crops to include potatoes and rapeseed (canola), both cold-tolerant, calorie-dense crops that are already widely cultivated globally and thus represent plausible replacement crops. To assess the potential for crop relocation to mitigate nuclear winter impacts, we implemented an optimization algorithm that identifies which of these six crops is the most productive under altered climate conditions for each location. The algorithm operates at the grid cell level, making relocation decisions in year 2 based on average yields projected for years 2-4 (representing the most acute phase, before production begins to recover around year 5). For each grid cell, we identify the crop with the highest caloric yield and evaluate whether existing agricultural areas should switch to this optimal choice. Switching occurs when the new crop's experience-adjusted yield exceeds both the current crop's yield and 500 kg/ha wheat equivalent (1.67 million kcal/ha). The true economically viable threshold would depend on complex factors including food prices, input costs, and labor availability during the crisis. We use 500 kg/ha as an illustrative threshold, approximately one-seventh of current global average wheat yields and comparable to late medieval UK production¹².

We account for farmer inexperience with new crops through yield penalties applied on top of climate-induced reductions: 40% additional reduction in the first year after switching, declining to 25% for the second year, then 10%, before full yields are achieved in the fourth year after switching. A study of conventional-to-organic farming transitions found first-year maize yields were approximately 60% of what farmers ultimately achieved after adapting to the organic system¹⁸. Though organic transition involves mainly system-wide changes rather than just crop-specific learning, both represent adaptation to unfamiliar production systems as well as changes in weed/pest ecology and soil nutrients. Similarly, US crop insurance for farmers with no growing records provides coverage at 65% of the county average yield, increasing gradually to 100% over three years¹⁹. While these analogies are imperfect, they suggest substantial but temporary yield reductions when farmers cultivate unfamiliar crops. The algorithm recognizes that grid cells contain multiple crop types, allowing some to switch while others maintain current cultivation of theoretically lower-yielding crops when inexperience penalties outweigh the potential gains.

In our primary analysis, we make relocation decisions only within cropland currently growing at least one of the six modeled crops, as these decisions require knowledge of both current and alternative crop yields

under nuclear winter conditions. We then apply the resulting percentage improvements to all global cropland as an approximation (but see **Expanding relocation to all global cropland**).

Fig. 2 illustrates the global caloric production under the three nuclear winter scenarios, comparing current planting patterns (solid lines) with optimized crop relocation (dashed lines). In relative terms, the 150 Tg scenario shows the greatest initial gains, with crop relocation approximately doubling caloric production in years 3 and 4. However, in absolute terms, the milder scenarios achieve larger improvements. In the 16 Tg scenario, relocation can lead to an improvement equivalent to more than 30% of baseline production from year 4 onward, while this number never exceeds 18% in the 150 Tg scenario. The shaded areas in Fig. 2 show uncertainty from varying our inexperience penalty assumptions by $\pm 50\%$. Even with increased penalties, crop relocation still provides substantial benefits from year 3 onward.

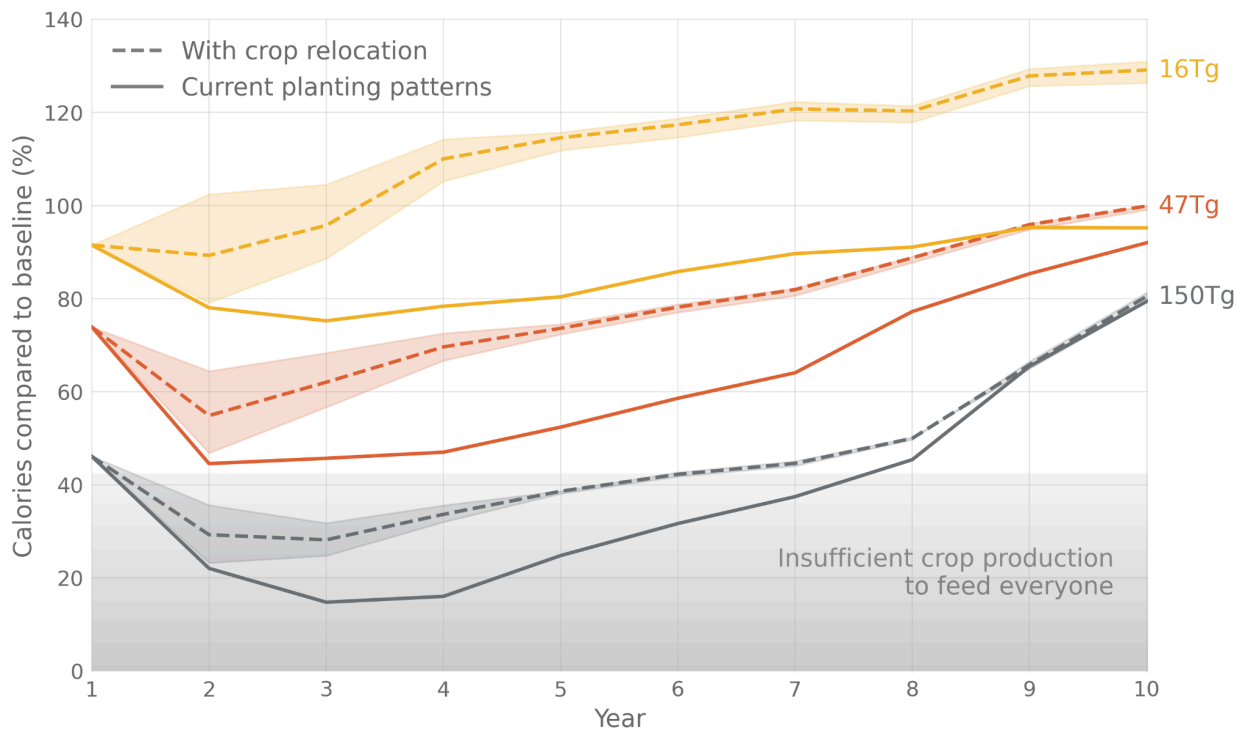


Fig. 2 | Global caloric production for maize, wheat, soybean, rice, potato and rapeseed with and without crop relocation. The plot shows calories produced compared to pre-war baseline levels (%). Solid lines represent current planting patterns, while dashed lines show results with optimal crop switching that maximizes caloric yield in each grid cell based on years 2-4 performance, accounting for inexperience penalties when farmers switch to unfamiliar crops (see text for details). Minor differences between the solid lines here and in Fig. 1 reflect the inclusion of potato and rapeseed alongside the four crops (maize, wheat, soybean, rice) analyzed in Fig. 1. Note that optimized production can exceed baseline levels in later years of mild scenarios because current agricultural systems are not purely optimized for caloric yield. Shaded areas represent uncertainty in the benefits of crop relocation due to farmer inexperience, calculated by varying the inexperience penalties by $\pm 50\%$ (multiplying baseline penalties by 0.5x for the lower bound and 1.5x for the upper bound).

The 16 Tg scenario's gains persist and even expand over time, while the 150 Tg scenario's benefits diminish as the climate recovers. This reflects the fact that crop distributions that maximize production during the acute phase of a severe nuclear winter (years 2-4) become increasingly suboptimal as

temperatures rebound. Since crop relocation occurs only once in our analysis (in year 2), these initially optimal configurations cannot adapt to changing conditions (subsequent relocations could further improve production in later years). In contrast, the more moderate climate perturbations of lighter soot scenarios allow for crop configurations that remain beneficial throughout the recovery period.

Even with crop relocation, the 150 Tg scenario remains below the 42% threshold for five years, still implying widespread famine would be unavoidable without additional measures beyond crop relocation and rationing food stocks.

Geographic patterns of food security Fig. 3 illustrates national self-sufficiency ratios (the ratio of domestically produced crop calories to population needs) under the assumption of no international food trade. Note that this analysis only considers crop-derived calories, excluding potential contributions from fisheries, grazing livestock, or other non-crop food sources. A ratio of 1.0 indicates a country has a crop production equivalent to 2,300 kcal per person per day. In the 16 Tg scenario, most nations maintain adequate self-sufficiency ratios even with current planting patterns. Many regions showing low self-sufficiency in the 16 Tg scenario (e.g., Japan, Korea, the Arabian Peninsula) already depend heavily on food imports under current conditions. In the 47 Tg scenario, food insecurity expands dramatically beyond current import-dependent nations. Major food exporters including the US, Canada, Russia and much of Europe fall below self-sufficiency thresholds without relocation. Crop relocation provides some relief (e.g., in the US), but still falls short of producing enough food to reach self-sufficiency in 85 countries representing 38% of the global population. The 150 Tg scenario shows near-total agricultural collapse across most of the Northern Hemisphere. Self-sufficiency ratios approach zero throughout North America, Europe, Russia, and China regardless of crop relocation, reflecting that extreme cooling renders temperate cropland non-productive for all modeled crops. Only South America, Oceania and equatorial regions maintain significant agricultural capacity.

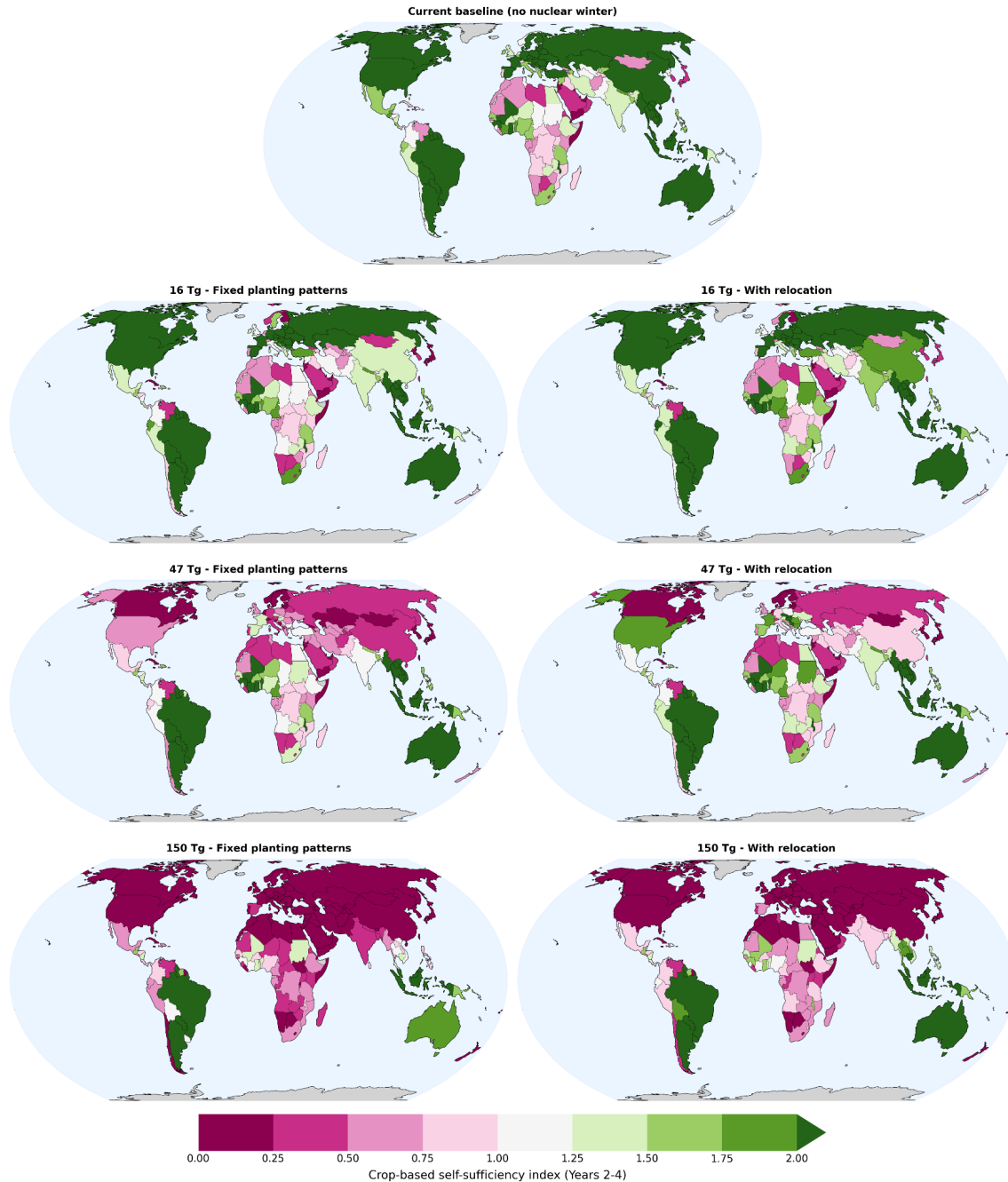


Fig. 3 | Crop-based self-sufficiency ratios by country for nuclear winter scenarios. Maps show the ratio of total available crop calories to population needs. The top panel displays current baseline self-sufficiency (no nuclear winter). The lower panels show three nuclear winter scenarios (16 Tg, 47 Tg, and 150 Tg) under two conditions: "Fixed planting patterns" (left column) and "With relocation" (right column). Self-sufficiency is calculated as the average over years 2-4 post-nuclear war for the nuclear winter scenarios. Fixed planting patterns represents baseline crop production⁵ adjusted for nuclear winter impacts on the six crops modeled in this work (maize, wheat, soybean, rice, potato, rapeseed). With relocation applies the improvement factors resulting from optimal crop switching that maximizes caloric yield in each grid cell. This analysis considers only crop-derived calories and assumes 10% food waste⁵ and that all human-edible crop production goes directly to human consumption (no animal feed or biofuel production).

Expanding relocation to all global cropland Our initial analysis could be underestimating the true potential of crop relocation because it implicitly assumes uniform percentage gains across all cropland. Our six modeled crops represent 51% of global cropland area (669 Mha out of 1320 Mha²⁰). The remaining 49% is predominantly planted with crops that are less calorie-dense than maize, wheat, soybean, rice, potato and rapeseed, including many crops with zero or minimal caloric contribution such as rubber, tobacco, coffee, and tea. Using historical yield data²⁰ and FAO caloric density values¹³, we calculate area-weighted average caloric yields of 16.9 million kcal/ha for our six modeled crops versus only 7.6 million kcal/ha for the 36 other crops included in the yield dataset. This difference in caloric yield means the potential gains from crop relocation are larger in the non-modeled cropland.

To explore this potential, we conducted an additional analysis where crop relocation is explicitly modeled across all non-tree cropland globally. We exclude tree crops such as oil palm, coconut, and fruit orchards from this analysis as converting these areas would require cutting down trees and extensive soil preparation, unlike transitions from other annual crops like sorghum, millet or beans where existing field infrastructure can be more readily adapted. However, we include tree crop caloric production by applying the nuclear winter yield reduction factors from Fig. 2 to current tree crop production levels, assuming tree crops experience similar relative yield declines as the staple crops under nuclear winter conditions. For this expanded analysis, we make the pessimistic assumption that the optimal replacement crop will always be one of our six modeled crops. This assumption is pessimistic because it means farmers switching from non-modeled crops will always incur the full inexperience penalty, whereas in reality some non-modeled crops might perform better than our six crops in specific locations under nuclear winter conditions.

Under this expanded relocation scenario, the results for the most severe 150 Tg case improve considerably. Global production maintains the critical threshold of 2,300 kcal/person/day in all years except years 2-4 (Extended Data Fig. 1). We do not present this expanded relocation as our primary scenario because converting all of the global cropland to maximize caloric production would likely be economically unrealistic, as demand for dietary diversity, industrial crops, nutritionally-rich energy-lean vegetables, animal products, and regional food preferences would persist even during a catastrophe. Nevertheless, this analysis demonstrates that significant additional food production potential exists within current agricultural land if calories are prioritized over crop diversity.

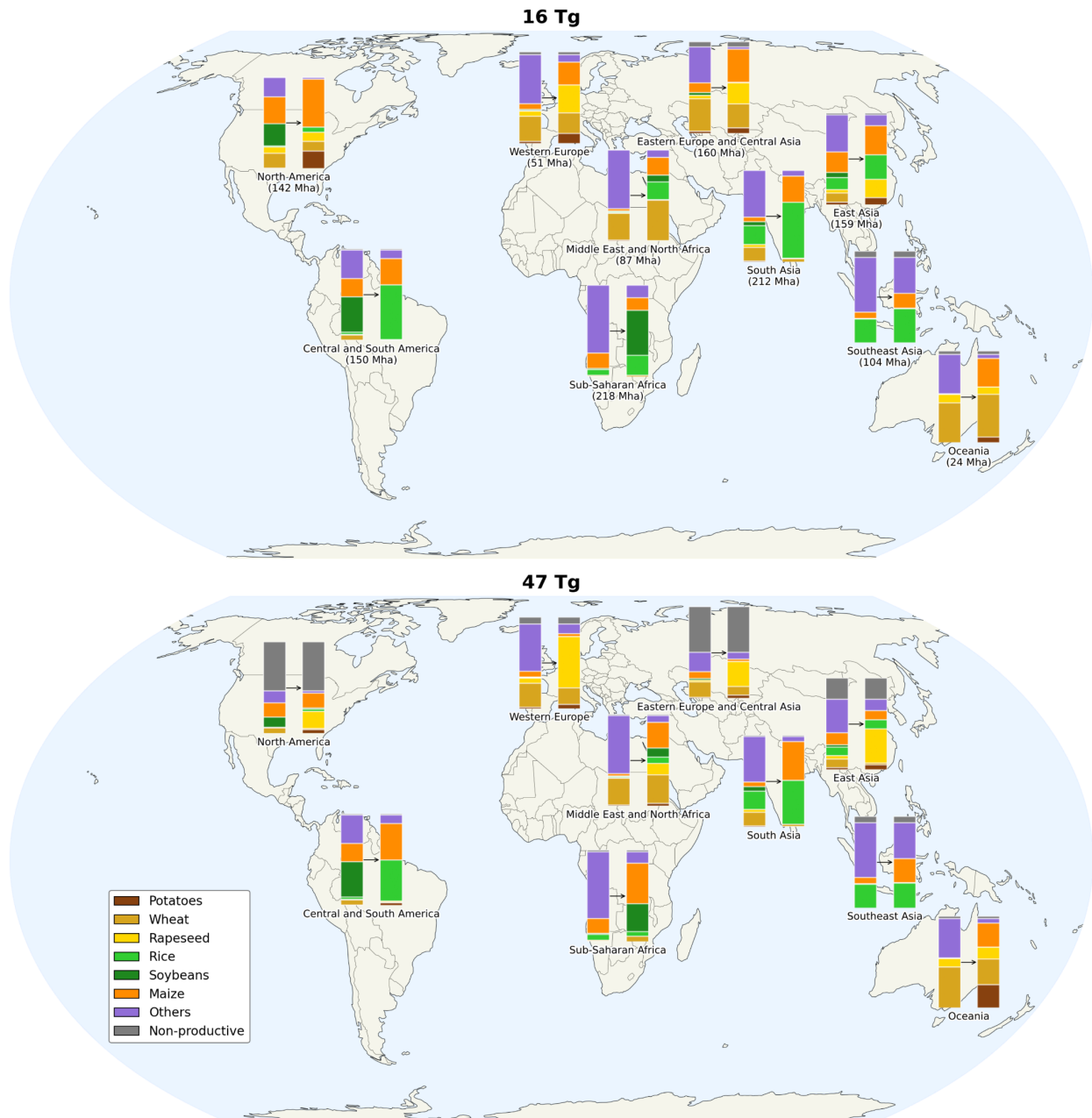
Regional cropland composition shifts Finally, we examine the crop relocation patterns at the regional level. Fig. 4 shows how the composition of cropland changes across different regions when we optimize for maximum caloric production, including relocation in areas currently growing crops not modeled in this study.

In the 16 Tg scenario, crop relocation patterns reflect optimization for caloric yield rather than cold tolerance. Under current growing conditions, rice and maize achieve the highest caloric yields among our modeled crops (24 and 23 million kcal/ha, respectively), substantially exceeding wheat (13 million kcal/ha), potato (15 million kcal/ha), soybean (10 million kcal/ha), and rapeseed (10 million kcal/ha)^{13,20}. Consequently, we observe major expansions of these warm-season crops wherever climate conditions permit. This shift is pronounced in North America, where maize expands from 29% to 51% of cropland area; in South America, where rice cultivation increases from 3% to 59%; and in South Asia, where rice expands from 20% to 60%. Note that rice expansion would not necessarily require flooded cultivation infrastructure as aerobic (non-flooded) rice systems can approach flooded yields^{21,22}.

The 47 Tg scenario reveals a split in relocation strategies between warmer and cooler regions. In South America, South Asia, and Sub-Saharan Africa, the shift toward rice and maize persists, driven by their superior caloric yields under conditions that remain warm enough for their cultivation. However,

temperate regions show markedly different patterns. North America, Europe, Central Asia, and East Asia experience substantial expansion of rapeseed cultivation, reflecting the need for cold-tolerant crops as temperatures drop below thresholds suitable for maize and rice. Large areas of cropland in Northern Hemisphere regions become non-productive in year 2, with none of our six modeled crops achieving yields above the 500 kg/ha wheat equivalent threshold.

Under the extreme 150 Tg scenario, crop relocation becomes impossible across vast areas of the Northern Hemisphere (see also Extended Data Fig. 2). North America, Europe, and a large portion of Asia show no viable relocation options, as extreme cooling renders these regions unsuitable for any of our modeled crops in year 2, consistent with the near-zero self-sufficiency ratios shown in Fig. 3. The remaining productive regions undergo compositional shifts toward cold-tolerant crops. Rapeseed expands significantly in South America and South Asia, while wheat becomes important in Sub-Saharan Africa.



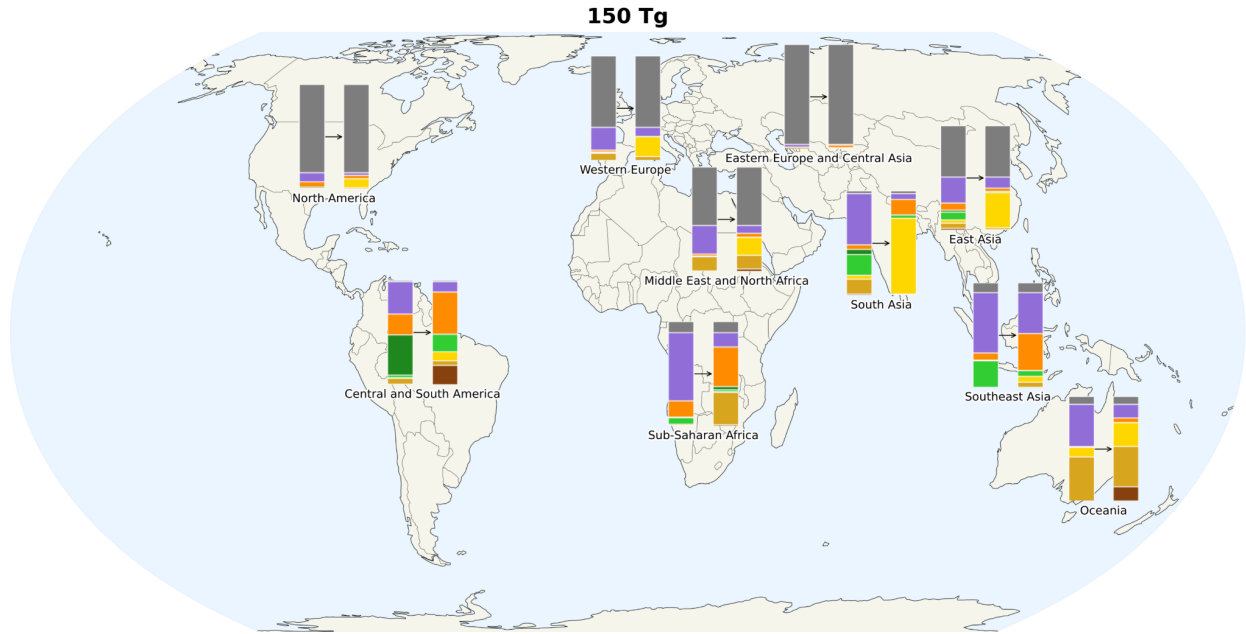


Fig. 4 | Regional crop area breakdown with and without crop relocation during nuclear winter. Bar charts display the composition of cropland area across different regions, comparing scenarios with and without crop relocation optimization (left and right, respectively). The analysis applies to all non-tree cropland globally, including the six crops modeled in this work (maize, wheat, soybean, rice, potato, rapeseed) as well as the cropland where crops not modeled in this work currently grow. Non-modeled crops are replaced by the best-performing modeled crop in each location. Non-productive areas (shown in gray) represent regions where none of the six modeled crops would achieve annual yields above the 500 kg/ha wheat equivalent threshold (approximately 1.67 million kcal/ha).

Discussion

Our results demonstrate that crop relocation could substantially mitigate nuclear winter's agricultural impacts, approximately doubling caloric production during the worst years of an extreme 150 Tg nuclear winter. This complements previous studies that assumed static crop distributions^{4,6,7} or only within-species cultivar selection^{8,9}. Optimal relocation strategies vary dramatically with cooling severity: mild scenarios (16 Tg) favor expanding high-calorie warm-season crops like rice and maize, while extreme scenarios (150 Tg) demand widespread conversion to cold-tolerant crops in any regions retaining agricultural viability.

While these findings demonstrate the value of agricultural preparedness, preventing nuclear war remains the only assured strategy to avoid these catastrophic outcomes. Despite the gains from crop relocation, it alone cannot prevent widespread famine in severe scenarios. Even with optimal implementation, the 150 Tg scenario remains below minimum caloric needs for several consecutive years, necessitating complementary strategies including improved food stock management⁵, non-agricultural food production systems^{23–26}, and agricultural expansion^{27–29}. Moreover, severe nuclear winter would concentrate global food production in tropical and Southern Hemisphere regions while rendering the Northern Hemisphere agriculturally non-viable. This geographic shift would require unprecedented coordination, with countries like Argentina, Brazil and Australia needing to expand exports massively to feed billions in regions that have lost productive capacity. Without such coordination and massive food transfers, regional famines would occur despite potentially adequate global production.

Future work should address several key areas to refine these findings. Many modeling assumptions require more research (Extended Data Table 1), including the magnitude of inexperience penalties, pest/disease responses, and fertilizer availability. Finer-scale regional analyses incorporating more detailed climate projections and infrastructure capacity would provide more actionable guidance for national planning. Controlled growth chamber experiments replicating nuclear winter conditions would help validate crop model predictions and reduce uncertainty in yield projections. Nutritional optimization should also be considered, as maximizing calories alone could cause protein, fat and micronutrient deficiencies³⁰. While our analysis focused on nuclear winter, the crop relocation approach may also apply to other abrupt cooling scenarios such as volcanic winter³¹, impact winter³², or rapid climate change events like Atlantic Meridional Overturning Circulation collapse³³. However, our quantitative results are specific to nuclear winter; other scenarios would require dedicated modeling to capture their distinct spatial and temporal characteristics.

This work has established crop relocation as an effective agricultural adaptation to nuclear winter, with benefits exceeding previous estimates⁵. Our findings suggest several preparedness priorities, including: (1) establishing seed reserves tailored to regional needs under different cooling scenarios; (2) developing crop transition training programs to minimize yield losses with unfamiliar species after crop switching; (3) negotiating advance food trade agreements between regions. While crop relocation alone cannot close the food production gap in extreme scenarios, these preparedness measures would significantly improve implementation speed and effectiveness if and when rapid adaptation becomes necessary.

Methods

Climate scenarios We used previously published climate projections from nuclear winter simulations^{2,4,34}, which were calculated using the Community Earth System Model with Whole Atmosphere Community Climate Model version 4 (CESM-WACCM4)³⁵. We considered three scenarios with stratospheric soot injections of 16, 47, and 150 Tg, representing a range of possible nuclear conflict scales and targeting strategies that result in global cropland mean temperature reductions reaching 4°C, 8°C, and 15°C in the worst year, respectively. The atmosphere and land have a horizontal resolution of 1.875° × 2.5° (latitude-longitude).

To address systematic biases in the climate model outputs, we applied the delta method for bias correction^{36,37}. This approach preserves the relative changes between nuclear winter and control simulations while anchoring absolute values to observed climatology. Specifically, we: (1) calculated monthly anomalies between nuclear winter and control runs from the WACCM4 simulations; (2) applied these anomalies to NASA POWER baseline climatology³⁸; and (3) generated daily weather sequences maintaining the observed variability patterns from the baseline period. While this method assumes unchanged climate variance, we deemed this an acceptable trade-off to correct systematic biases, including precipitation overestimations exceeding 100% in some regions for baseline climate³⁹.

Crop modeling framework We employed the Mink global gridded crop modeling system⁴⁰, built on version 4.7 of the Decision Support System for Agrotechnology Transfer (DSSAT) framework^{41,42}. As a process-based model, Mink simulates crop growth through mechanistic representations of photosynthesis, respiration, phenology, and water/nutrient dynamics. This approach enables more reliable extrapolation to the unprecedented conditions of nuclear winter compared to statistical models trained on historical data.

Simulations were conducted at $1.875^\circ \times 1.25^\circ$ resolution for six major crops: maize, wheat (spring and winter varieties), soybean, rice, potato, and rapeseed. For all scenarios, we optimized planting dates by simulating each crop with twelve possible planting months and selecting the month yielding the highest output for each year independently. Crops were always planted on the first day of the month. This strategy maintains reasonably close yield patterns to current crop yields in baseline conditions, and assumes farmers would adapt to the nuclear winter by planting in the best yielding month. Soil properties were derived from the global SoilGrids database⁴³, while current crop distributions and irrigated versus rainfed classifications followed the SPAM 2020 datasets²⁰. Irrigated crops are simulated assuming no water stress. Our analysis excludes fodder cropland and fallow land not captured in SPAM 2020, representing approximately 17% of global agricultural land that could potentially be converted to food crop production during a crisis. Fertilizer application rates were held constant at current levels based on FAO statistics⁴⁴. This assumption is optimistic given likely supply chain disruptions after a nuclear conflict^{45,46}. However, the reduction in viable cropland could partially offset supply constraints by concentrating remaining fertilizer on a smaller cultivated area.

Cultivar selection For all crops except soybean and wheat, we maintained fixed cultivar assignments based on current planting patterns, without optimization for nuclear winter climates. For wheat and potatoes, we employed an existing Mega Environment (ME) classification system^{44,47}. In grid cells where multiple MEs overlap, yields were averaged across cultivars. For wheat, the highest yielding cultivars were selected for Western European countries in baseline as well as nuclear winter scenarios. This strategy has been shown to replicate current-day yield patterns⁴⁴. Maize cultivars followed the same ME-based approach using current climate classifications. Rice simulations used either indica or japonica varieties based on the predominant type currently grown in each grid cell. For rapeseed, all simulations used the InVigor 5440 canola variety. For soybean, we independently selected the highest-yielding maturity group for each grid cell in baseline and nuclear winter scenarios, replicating current maturity group distributions in the baseline while allowing within-species adaptation under nuclear winter.

Simulation scenarios We conducted three sets of simulations to evaluate crop relocation potential under nuclear winter conditions. The first set consists of the control runs used to establish baseline yields with NASA POWER climate data from 2001-2009 and current crop distributions from SPAM 2020. After a two-year model stabilization period (2001-2002), we calculated average yields over seven years (2003-2009) to account for inter-annual variability and provide a robust baseline for comparison. The second set consists of the base nuclear winter runs, where we maintained current crop distributions while applying climate perturbations from the 16, 47, and 150 Tg soot injection scenarios. These simulations included a two-year acclimatization period using the control climate data, followed by ten years of

nuclear winter conditions. Finally, for the third set we considered all grid cells that contain cropland and simulated all six crops in each grid cell. This resulted in at least 72 simulations per grid cell (6 crops × 12 months). The actual number of simulations per grid cell was in fact higher due to the inclusion of multiple cultivars.

Crop yield bias adjustment To ensure accurate inter-species comparisons essential for crop relocation decisions, we calibrated our modeled yields against observed production data. We compared our baseline simulation results to FAO global production statistics for 2020 for all six crops (Extended Data Table 2)⁴⁸. While some crops showed good agreement (global maize production was within 8% of FAO values), others exhibited substantial biases (potato yields were overestimated by 50%). These discrepancies likely arise from limitations in capturing management practices, cultivar diversity, or pests and diseases. We calculated global crop-specific correction factors as the ratio between FAO-reported and modeled production to adjust for these systematic biases. These correction factors were applied to all simulation results across all scenarios. While this adjustment does not affect relative yield changes within a single crop (e.g., the percentage decline in wheat production under nuclear winter), it is crucial for absolute yield comparisons between different crop species when determining optimal crop allocation strategies. Accurate absolute yields are also essential for calculating whether global production can sustain the population.

We did not explicitly model more than one crop harvest per year. However, our crop yield bias adjustment against FAO production statistics implicitly captures current multiple cropping practices in baseline yields. Under nuclear winter conditions, shortened growing seasons would likely eliminate double cropping in many regions where it is currently practiced, potentially causing our approach to underestimate yield losses. However, the magnitude of this underestimation is bounded: global cropping intensity (harvested area/cropland area, excluding fallow land) is 1.13⁴⁹, meaning that there is currently only 13% more harvested area than land area. Even if nuclear winter completely eliminated all multiple cropping worldwide, the impact on our global results would therefore be limited to approximately this percentage.

Verifications with a second crop model To verify the robustness of our findings, we conducted parallel simulations using version 2024.10.7600.0 of the Agricultural Production Systems sIMulator (APSIM)^{50,51}. While our maize, wheat, soybean, and rice results aligned well with Xia et al.'s projections for current cropland distributions, we are not aware of existing nuclear winter results for potatoes and rapeseed, making independent model verification particularly valuable.

For these verification runs, we standardized conditions to ensure model comparability: simulating rainfed agriculture only, using a single cultivar per crop, and assuming no nitrogen stress in both DSSAT and APSIM models. We simulated planting each crop (potatoes and rapeseed) across all grid cells where any of our six modeled crops are currently grown, using identical climate data and soil properties as in the DSSAT simulations. We applied the same crop yield bias adjustment methodology to APSIM, calculating correction factors by comparing the APSIM baseline global yields to FAO 2020 production data.

The results provided mixed validation. Rapeseed yields showed strong agreement between models, with APSIM projecting 488 Mt/yr averaged over years 2-4 compared to DSSAT's 440 Mt/yr. However, potato yields diverged substantially, with APSIM projecting 709 Mt/yr versus DSSAT's 371 Mt/yr. While this discrepancy raises questions about model uncertainty, our use of the more conservative DSSAT projections helps us to avoid overstating the potential benefits of potato relocation. These findings highlight the need for systematic crop model intercomparison exercises under extreme climate conditions. Nuclear winter scenarios push models beyond their calibration range, and controlled experiments replicating low-light, cold conditions would help benchmark model performance in this unique regime.

Code Availability

The Mink global gridded crop model is available at <https://github.com/allfed/mink/tree/1.0>. The DSSAT code and executable used for crop model runs may be found at <https://github.com/morganrivers/dssat-csm-os/releases/tag/1.0>.

Data Availability

All data used to run the crop models and simulation results for all crops are located at <https://zenodo.org/records/16940939>. This includes weather data for all scenarios, 2020 SPAM crop yields and currently grown species areas for irrigated and rainfed crops, nitrogen application rates, soil types, cultivar maps, land area, soil carbon maps, and country boundaries.

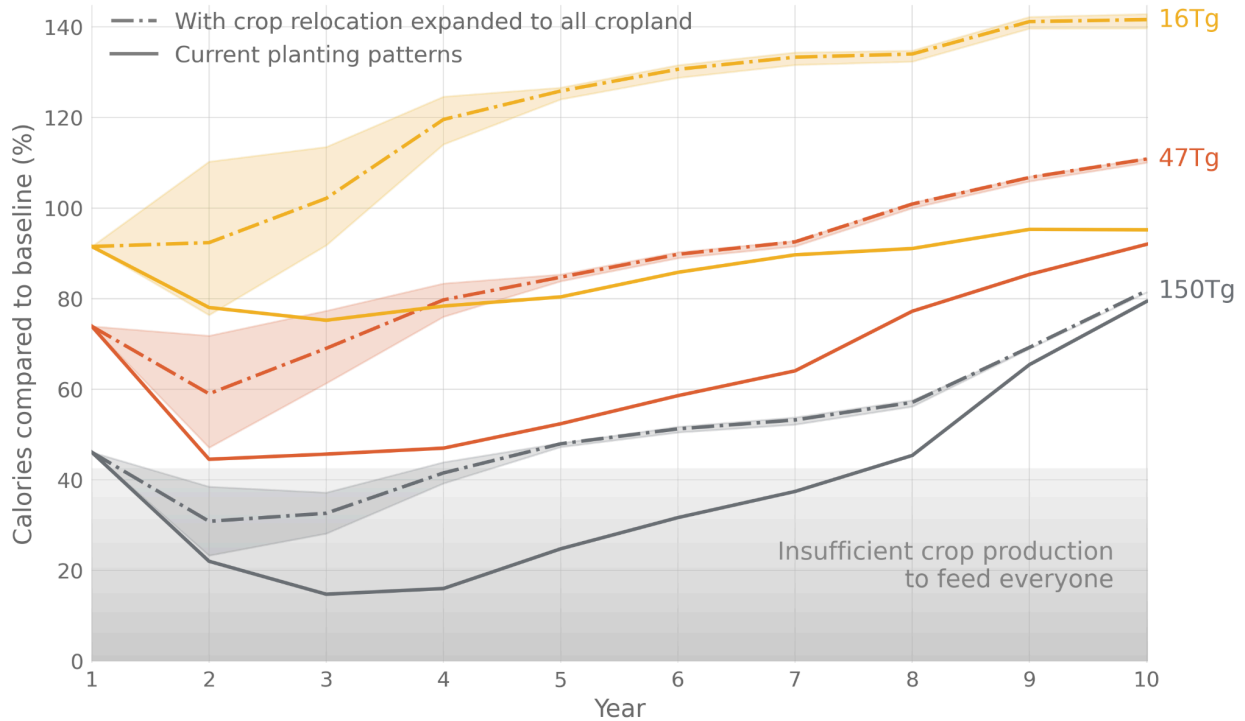
Acknowledgements

The authors thank Juan García for his feedback on the manuscript and Lili Xia for sharing climate simulation data.

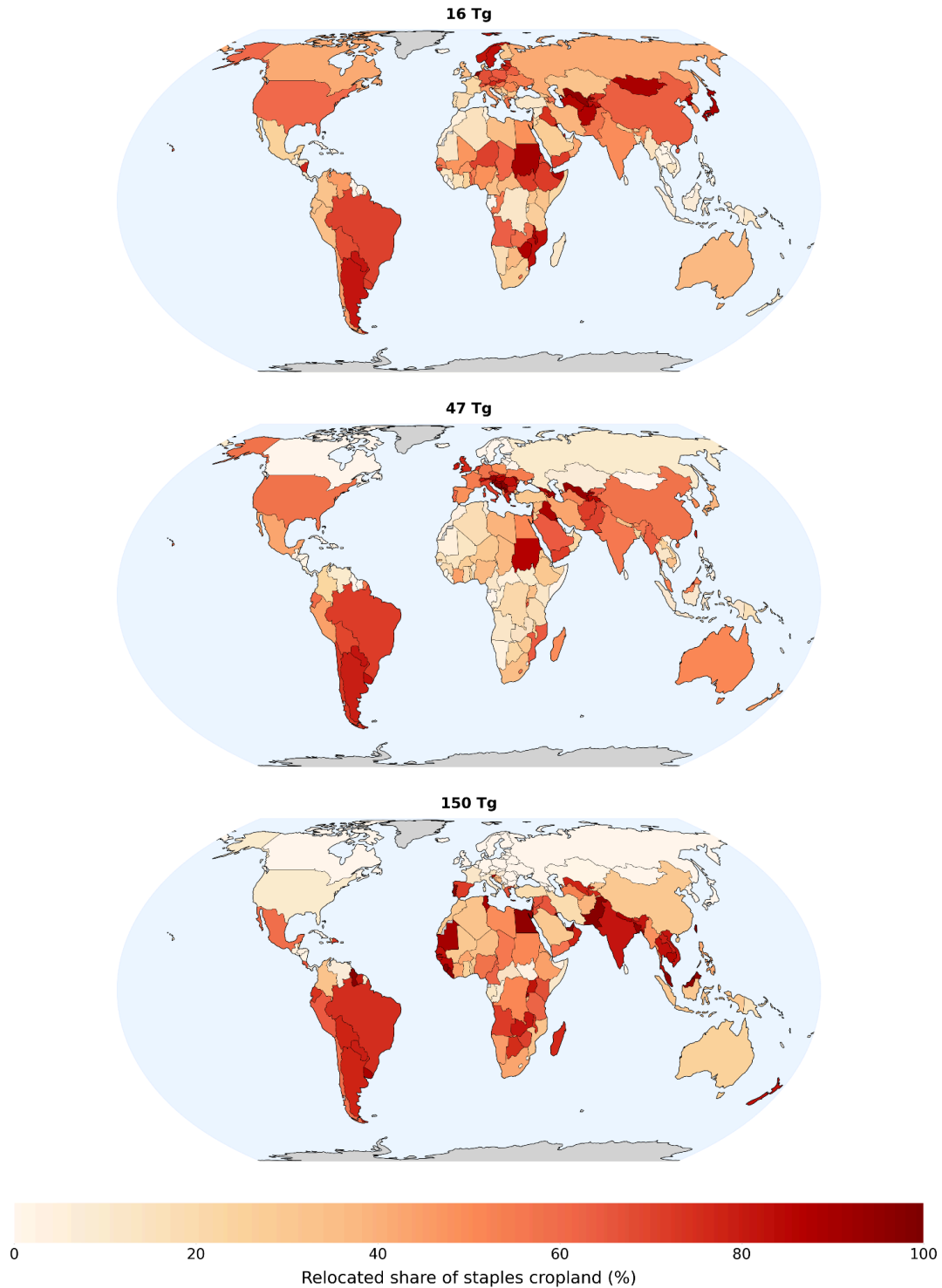
References

1. Robock, A., Oman, L. & Stenchikov, G. L. Nuclear winter revisited with a modern climate model and current nuclear arsenals: Still catastrophic consequences. *J. Geophys. Res. Atmospheres* **112**, 2006JD008235 (2007).
2. Coupe, J., Bardeen, C. G., Robock, A. & Toon, O. B. Nuclear Winter Responses to Nuclear War Between the United States and Russia in the Whole Atmosphere Community Climate Model Version 4 and the Goddard Institute for Space Studies ModelE. *J. Geophys. Res. Atmospheres* **124**, 8522–8543 (2019).
3. National Academies of Sciences, Engineering, and Medicine, Committee on Independent Study on Potential Environmental Effects of Nuclear War, Board on Atmospheric Sciences and Climate, Nuclear and Radiation Studies Board, & Division on Earth and Life Studies. *Potential Environmental Effects of Nuclear War*. (National Academies Press, Washington, D.C., 2025). doi:10.17226/27515.
4. Xia, L. *et al.* Global food insecurity and famine from reduced crop, marine fishery and livestock production due to climate disruption from nuclear war soot injection. *Nat. Food* **3**, 586–596 (2022).
5. Rivers, M. *et al.* Food System Adaptation and Maintaining Trade Could Mitigate Global Famine in Abrupt Sunlight Reduction Scenarios. *Glob. Food Secur.* **43**, (2024).
6. Özdoğan, M., Robock, A. & Kucharik, C. J. Impacts of a nuclear war in South Asia on soybean and maize production in the Midwest United States. *Clim. Change* **116**, 373–387 (2013).
7. Jägermeyr, J. *et al.* A regional nuclear conflict would compromise global food security. *Proc. Natl. Acad. Sci.* **117**, 7071–7081 (2020).
8. McLaughlin, C. M. *et al.* Maladaptation in cereal crop landraces following a soot-producing climate catastrophe. *Nat. Commun.* **16**, (2025).
9. Shi, Y. *et al.* Adapting agriculture to climate catastrophes: the nuclear winter case. *Environ. Res. Lett.* **20**, 064006 (2025).
10. Nunn, N. & Qian, N. The Potato's Contribution to Population and Urbanization: Evidence From A Historical Experiment*. *Q. J. Econ.* **126**, 593–650 (2011).
11. Sloat, L. L. *et al.* Climate adaptation by crop migration. *Nat. Commun.* **11**, 1243 (2020).
12. Ritchie, H., Rosado, P. & Roser, M. Agricultural Production. *OurWorldinData.org* <https://ourworldindata.org/agricultural-production> (2023).
13. FAO. *FAO Food Balance Sheets: A Handbook*. (2001).
14. Alexander, P. *et al.* Losses, inefficiencies and waste in the global food system. *Agric. Syst.* **153**, 190–200 (2017).
15. WHO. *The Management of Nutrition in Major Emergencies*. (World Health Organization, 2000).
16. Laio, F., Ridolfi, L. & D'Odorico, P. The past and future of food stocks. *Environ. Res. Lett.* **11**, 035010 (2016).
17. Martin, W. & Anderson, K. Export Restrictions and Price Insulation During Commodity Price Booms. *Am. J. Agric. Econ.* **94**, 422–427 (2012).
18. Caldwell, B., Mohler, C. L., Ketterings, Q. M. & DiTommaso, A. Yields and Profitability during and after Transition in Organic Grain Cropping Systems. *Agron. J.* **106**, 871–880 (2014).
19. USDA. Common Crop Insurance Policy Basic Provisions. (2024).
20. Institute (IFPRI), I. F. P. R. Global Spatially-Disaggregated Crop Production Statistics Data for 2020 Version 2.0. Harvard Dataverse <https://doi.org/10.7910/DVN/SWPENT> (2025).
21. Peng, S. *et al.* Comparison between aerobic and flooded rice in the tropics: Agronomic performance in an eight-season experiment. *Field Crops Res.* **96**, 252–259 (2006).
22. Patel, D. P. *et al.* Evaluation of yield and physiological attributes of high-yielding rice varieties under aerobic and flood-irrigated management practices in mid-hills ecosystem. *Agric. Water Manag.* **97**, 1269–1276 (2010).
23. Jehn, F. U. *et al.* Seaweed as a Resilient Food Solution After a Nuclear War. *Earths Future* **12**, e2023EF003710 (2024).
24. Hinge, M. *et al.* Seaweed cultivation: a cost-effective strategy for food production in a global catastrophe. *Aquac. Int.* **33**, (2025).
25. García Martínez, J. B. *et al.* Methane Single Cell Protein: Potential to Secure a Global Protein Supply Against Catastrophic Food Shocks. *Front. Bioeng. Biotechnol.* **10**, 906704 (2022).
26. Throup, J. *et al.* Rapid repurposing of pulp and paper mills, biorefineries, and breweries for lignocellulosic sugar production in global food catastrophes. *Food Bioprod. Process.* **131**, 22–39 (2022).
27. Alvarado, K. A., Mill, A., Pearce, J., Vocaet, A. & Denkenberger, D. Scaling of greenhouse crop production in low sunlight scenarios. *Sci. Total Environ.* **707**, 136012 (2020).
28. Boyd, M. & Wilson, N. Resilience to abrupt global catastrophic risks disrupting trade: Combining urban and near-urban agriculture in a quantified case study of a globally median-sized city. *PLOS One* **20**, e0321203 (2025).
29. Monteiro, L. *et al.* Expansion of cropland area during an abrupt sunlight reduction scenario. Preprint at

- <https://doi.org/10.31223/X5MQ54> (2024).
30. Pham, A. *et al.* Nutrition in Abrupt Sunlight Reduction Scenarios: Envisioning Feasible Balanced Diets on Resilient Foods. *Nutrients* **14**, 492 (2022).
 31. Robock, A. Volcanic eruptions and climate. *Rev. Geophys.* **38**, 191–219 (2000).
 32. Toon, O. B., Zahnle, K., Morrison, D., Turco, R. P. & Covey, C. Environmental perturbations caused by the impacts of asteroids and comets. *Rev. Geophys.* **35**, 41–78 (1997).
 33. Jackson, L. C. *et al.* Global and European climate impacts of a slowdown of the AMOC in a high resolution GCM. *Clim. Dyn.* **45**, 3299–3316 (2015).
 34. Toon, O. B. *et al.* Rapidly expanding nuclear arsenals in Pakistan and India portend regional and global catastrophe. *Sci. Adv.* **5**, eaay5478 (2019).
 35. Hurrell, J. W. *et al.* The Community Earth System Model: A Framework for Collaborative Research. (2013) doi:10.1175/BAMS-D-12-00121.1.
 36. Hawkins, E., Osborne, T. M., Ho, C. K. & Challinor, A. J. Calibration and bias correction of climate projections for crop modelling: An idealised case study over Europe. *Agric. For. Meteorol.* **170**, 19–31 (2013).
 37. Laux, P. *et al.* To bias correct or not to bias correct? An agricultural impact modelers' perspective on regional climate model data. *Agric. For. Meteorol.* **304–305**, 108406 (2021).
 38. Zhang, T. *et al.* A Global Perspective on Renewable Energy Resources: Nasa's Prediction of Worldwide Energy Resources (Power) Project. in *Proceedings of ISES World Congress 2007 (Vol. I – Vol. V)* (eds. Goswami, D. Y. & Zhao, Y.) 2636–2640 (Springer, Berlin, Heidelberg, 2009). doi:10.1007/978-3-540-75997-3_532.
 39. Liu, Z., Mehran, A., Phillips, T. J. & AghaKouchak, A. Seasonal and regional biases in CMIP5 precipitation simulations. *Clim. Res.* **60**, 35–50 (2014).
 40. Robertson, R. D. *Mink: Details of a Global Gridded Crop Modeling System*. (International Food Policy Research Institute (IFPRI), Washington, D.C., 2017).
 41. Jones, J. W. *et al.* The DSSAT cropping system model. *Eur. J. Agron.* **18**, 235–265 (2003).
 42. Hoogenboom, G. *et al.* The DSSAT crop modeling ecosystem. in *Advances in crop modelling for a sustainable agriculture* (ed. Boote, K.) (Burleigh Dodds Science Publishing, London, 2019).
 43. Han, E., Ines, A. V. M. & Koo, J. Development of a 10-km resolution global soil profile dataset for crop modeling applications. *Environ. Model. Softw.* **119**, 70–83 (2019).
 44. Gbegbelegbe, S. *et al.* Baseline simulation for global wheat production with CIMMYT mega-environment specific cultivars. *Field Crops Res.* **202**, 122–135 (2017).
 45. Moersdorf, J., Rivers, M., Denkenberger, D., Breuer, L. & Jehn, F. U. The Fragile State of Industrial Agriculture: Estimating Crop Yield Reductions in a Global Catastrophic Infrastructure Loss Scenario. *Glob. Chall.* **8**, 2300206 (2024).
 46. Blouin, S., Jehn, F. U. & Denkenberger, D. Global industrial disruption following nuclear war. Preprint at <https://doi.org/10.31223/X58H9G> (2024).
 47. Raymundo, R. *et al.* Climate change impact on global potato production. *Eur. J. Agron.* **100**, 87–98 (2018).
 48. FAOSTAT. Crops and livestock products. <https://www.fao.org/faostat/en/#data/QCL>.
 49. Waha, K. *et al.* Multiple cropping systems of the world and the potential for increasing cropping intensity. *Glob. Environ. Change* **64**, 102131 (2020).
 50. Holzworth, D. P. *et al.* APSIM – Evolution towards a new generation of agricultural systems simulation. *Environ. Model. Softw.* **62**, 327–350 (2014).
 51. Holzworth, D. *et al.* APSIM Next Generation: Overcoming challenges in modernising a farming systems model. *Environ. Model. Softw.* **103**, 43–51 (2018).
 52. Rosenzweig, C., Iglesias, A., Yang, X. B., Epstein, P. R. & Chivian, E. Climate Change and Extreme Weather Events; Implications for Food Production, Plant Diseases, and Pests. *Glob. Change Hum. Health* **2**, 90–104 (2001).
 53. Singh, B. K. *et al.* Climate change impacts on plant pathogens, food security and paths forward. *Nat. Rev. Microbiol.* **21**, 640–656 (2023).
 54. Mills, M. J., Toon, O. B., Turco, R. P., Kinnison, D. E. & Garcia, R. R. Massive global ozone loss predicted following regional nuclear conflict. *Proc. Natl. Acad. Sci.* **105**, 5307–5312 (2008).



Extended Data Fig. 1 | Global caloric production for maize, wheat, soybean, rice, potato and rapeseed if crop relocation is performed over all non-tree cropland. The plot shows calories produced compared to pre-war baseline levels (%) over a 10-year period for three soot injection scenarios: 150 Tg (gray), 47 Tg (orange), and 16 Tg (yellow). Solid lines represent current planting patterns, while dashed lines show results with optimal crop relocation expanded to all non-tree cropland globally, including areas currently growing non-tree crops not modeled in this work. Tree crop calories are included in both scenarios by applying the nuclear winter yield reduction factors from Fig. 2 to current tree crop production. Shaded areas represent uncertainty bounds from varying inexperience penalties by $\pm 50\%$, with the upper bound of the shaded area showing results with reduced penalties (0.5x multiplier) and the lower bound showing results with increased penalties (1.5x multiplier).



Extended Data Figure 2 | Geographic distribution of crop relocation intensity. Maps show the percentage of staple cropland area that would undergo crop switching in each country under three nuclear winter scenarios. Values represent the relocation share calculated as the fraction of cropland currently growing one of the six modeled crops (maize, wheat, soybean, rice, potato, rapeseed) that would switch to a different crop under the optimization strategy. Light colors in the 150 Tg scenario across the Northern Hemisphere reflect that most cropland becomes non-productive.

Extended Data Table 1 | Summary of modeling assumptions and their directional bias on food production estimates

Assumption	Directional bias	Justification
Crop management and farmer adaptation		
Farmers plant at near-optimal dates each year (planting month optimized)	Unknown	Assumes perfect information; but our model optimizes on a monthly timestep whereas real farmers make finer adjustments; net effect uncertain
Inexperience penalty of 40% on the first year post-relocation declining gradually to 0% over 3 years	Unknown	Limited empirical basis
No subsequent relocation after year 2	Pessimistic	Farmers would likely continue optimizing as conditions change
Fixed cultivars for maize, rice, potato, rapeseed	Pessimistic	Within-species adaptation could improve yields ^{8,9}
Multiple cropping intensity maintained at current levels	Optimistic	Shortened growing seasons and longer crop cycles would likely eliminate double cropping
Relocation limited to six modeled crops	Pessimistic	Other cold-tolerant crops might perform better in some regions
No relocation on fodder cropland, fallow land or tree cropland	Pessimistic	Excludes ~25% of cropland (17% from fodder cropland and fallow land, 8% from tree cropland)
No expansion of agricultural land or urban agriculture	Pessimistic	Emergency cultivation of marginal lands likely ^{28,29}
1.67 million kcal/ha threshold for cropland conversion	Unknown	Actual threshold depends on future prices and costs
Agricultural inputs and infrastructure		
Adequate seed availability for alternative crops	Optimistic	Seed supply chains likely disrupted; existing reserves may be insufficient
Fertilizer application rate per unit area maintained at current levels	Optimistic	Supply chain disruptions likely, but reduced cropland area could partially offset this
Diesel, pesticides and machinery parts remain available	Optimistic	Supply chain disruptions likely

No water stress in irrigated cropland	Optimistic	Represents an upper bound on irrigated cropland productivity
Biophysical and environmental constraints		
No change in pest and disease pressure	Unknown	Competing effects: cold may reduce pest overwinter survival and slow pathogen cycles ^{52,53} , but stressed crops may be more susceptible and increased relative humidity would promote disease pressure; crop relocation could escape current pests or encounter new ones; net effect unknown
UV-B radiation effects ⁵⁴ excluded	Optimistic	UV damage peaks Years 6-8 (~7% maize reduction ⁹), well after critical food bottleneck of Years 2-4 when soot absorption actually reduces UV
Cropland outside immediate blast zones is unaffected by fallout or social disruption	Optimistic	Ignores potential radionuclide contamination or market collapse
Methodological simplifications		
Yield-bias factors derived from FAO data remain valid under nuclear winter conditions	Unknown	Extrapolates historical relative performance
Delta-method bias correction preserves inter-annual yield variability	Unknown	Unclear what is the net effect of holding climate variance constant

Extended Data Table 2 | Comparison of modeled baseline production with FAO statistics

Crop	Modeled baseline (Mt)	FAO 2020 observed (Mt)
Maize	1247	1155
Potato	562	369
Rapeseed	54	72
Rice	590	775
Soy	499	356
Wheat	979	760